Supporting Information

A Possible Mechanism for the Emergence of Additional Band Gap due to Ti-O-C Bond in TiO_2 - Graphene Hybrid System for Enhanced Photodegradation of Methylene Blue under Visible Light

Sima Umrao[†, #], Shiju Abraham[†, #, £, ‡], Frank Theil[£, ‡], Shobhit Pandey[¥], Valerian Ciobota[£], P. K. Shukla[€], Caroline J Rupp,[θ] Sudip Chakraborty,[λ] Rajeev Ahuja,[λ] Jürgen Popp[£, ‡], Benjamin Dietzek[£, ‡,*], Anchal Srivastava[†,*]

[†] Department of Physics, Banaras Hindu University, Varanasi, 221005, India.

[£] Institute of Physical Chemistry and Abbe Center of Photonics, Friedrich-Schiller-University, Helmholtzweg 4, D-07743, Jena, Germany.

[‡] Leibniz-Institute of Photonic Technology Jena (IPHT), Albert-Einstein-Str. 9, D-07745, Jena, Germany.

[¥] Metallurgical Engineering Department, Indian Institute of Technology-B. H. U., Varanasi, 221005, India.

[€] I.T.S. Engineering College, Greater Noida, 201308, India

[θ]Departamento de Física, Universidade Federal de Santa Maria, 97105-900, Santa Maria, RS, Brazil.

[λ]Condensed Matter Theory Group, Department of Physics and Astronomy, Uppsala University, Box-516, Sweden

[*] **Corresponding authors:**

Address correspondence to anchalbhu@gmail.com, benjamin.dietzek@ipht-jena.de

XRD Diffraction Pattern.

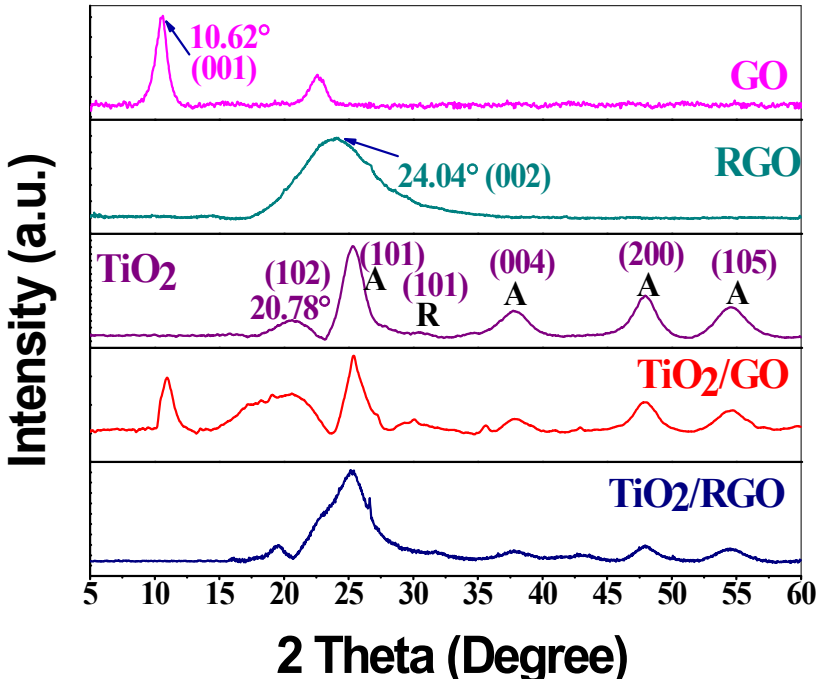

Figure S1. XRD patterns of GO, RGO, TiO_2, TiO_2: GO (TG), and TiO_2: RGO (TR).

Raman Spectrum and Interpretation.

Raman spectroscopy is a fast and non-destructive technique to distinguish between sp^2 and sp^3 hybridization in carbonaceous materials.[1-3] The G-band and D-band are the two main characteristic Raman bands observed in almost all carbon-based materials which are originating from the doubly degenerate zone center E_{2g} vibrational mode of sp^2 bonded carbon atoms and from the disorder respectively.[2] The results of Raman measurements of GO, RGO, TiO_2, TG and TR of the present investigations are depicted in Figure S1. From Fig. S1a the peak positions of GO are observed at 1350 cm^{-1} (D-band) and 1599 cm^{-1} (G-band). Furthermore the I_D/I_G ratio (which is a sensitive measure of the disorder) obtained in our case is 1.3. This relatively high value is an indication of higher level of oxidation and thus the presence of more functional groups in the synthesized GO. RGO reveals Raman peaks 1346 cm^{-1} and 1590 cm^{-1} respectively for D- and G-bands. Here the red shift in wavenumber in comparison to GO or moving more towards the graphitic edge is an indication of its reduction from GO. The I_D/I_G ratio is reduced to 1.18 in the case of RGO, which is less than that of GO. This observation is supported by the fact that the ratio of sp^3 to sp^2 hybridization decreases when GO

reduces to RGO.[3] The Raman spectrum of TiO_2 nanopowder is presented in Fig S1b. The peaks observed around 148, 267, 402, 514 and 638 cm^{-1} are assigned to the $E_{(g)}$, $E_{(g)}$, $B_{(1g)}$, $B_{(1g)}$+ $A_{(1g)}$, and the $E_{(g)}$ modes of anatase phases respectively.[4] The spectra of TG and TR are presented in Fig S1b. In TG1 and TG2, the peak positions shows a redshift in D-band (1343, 1340 cm^{-1}) and in G-band (1594, 1594 cm^{-1}) in comparison to GO. And the I_D/I_G ratio of TG1and TG2 increases to 1.54 and 1.42 respectively. These shifts may be attributed to the photo-thermal reduction of GO as well as the increased disorder upon the attachment of TiO_2 nanopowder. While in the case of TR1 and TR2 there is only a small change in peak positions (~3 cm^{-1}), but the disorder increases to 1.55 and 1.59 respectively. These observations are also justifiable in the sense of its already much reduced status and increased disorder in the graphitic nature due to the decoration of TiO_2 nanopowder. So the Raman investigation studies support the successful synthesis of GO, RGO, TiO_2, TG and TR.

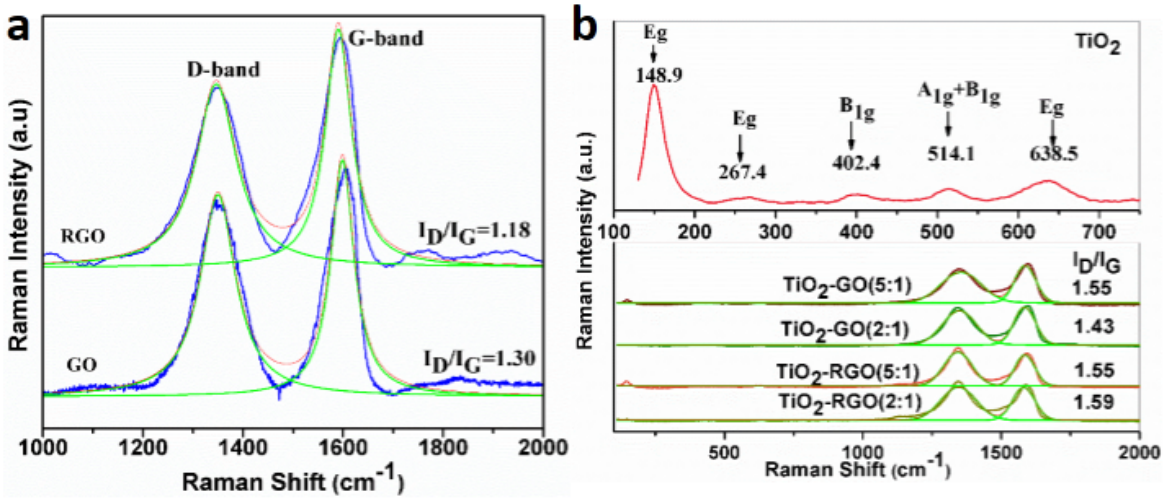

Figure S2. (a) Raman patterns of GO and RGO and (b) Raman patterns of TiO_2, TiO_2-GO (TG) and TiO_2-RGO (TR) of different concentration.

FT-IR Spectra and Analysis.

Fourier transform infrared (FT-IR) spectra of the synthesized TiO_2 nanopowder, TG and TR composite are shown in Figure S2. The spectra of TiO_2 shows a broad band around 500 cm^{-1}, which is attributed to the Ti−O−Ti stretching mode. The O−H stretching frequency from the surface hydroxyl groups is observed around 3400 cm^{-1}. The spectra also show a broad band at 1383 cm^{-1} due to organic residues

originating from the sample as a result of synthesis procedure.[5] In the spectrum of TG and TR, the absorption band at 1631 cm^{-1} results from the skeletal vibration of the graphene sheets. The other FT-IR absorption bands of TG include bands at 3410 cm^{-1} (O–H stretching vibration), 1393 cm^{-1} (C=O stretching vibrations) and 1079 cm^{-1} (C–O stretching vibrations),[6] which were decreased dramatically in intensity or even disappeared in comparison to the same bands of TR. The broad peak around 500 cm^{-1} in the FT-IR spectrum of TG and TR is shifted more towards higher wavenumbers and much broader than TiO_2. This peak originates from the combination of Ti-O-Ti vibrations and Ti-O-C vibrations.[7] During the mixing of GO and RGO with TiO_2 nanopowder, the residual carboxylic groups interact with the surface hydroxyl groups of TiO_2 nanopowder and form the chemically bonded TG and TR composites.[8]

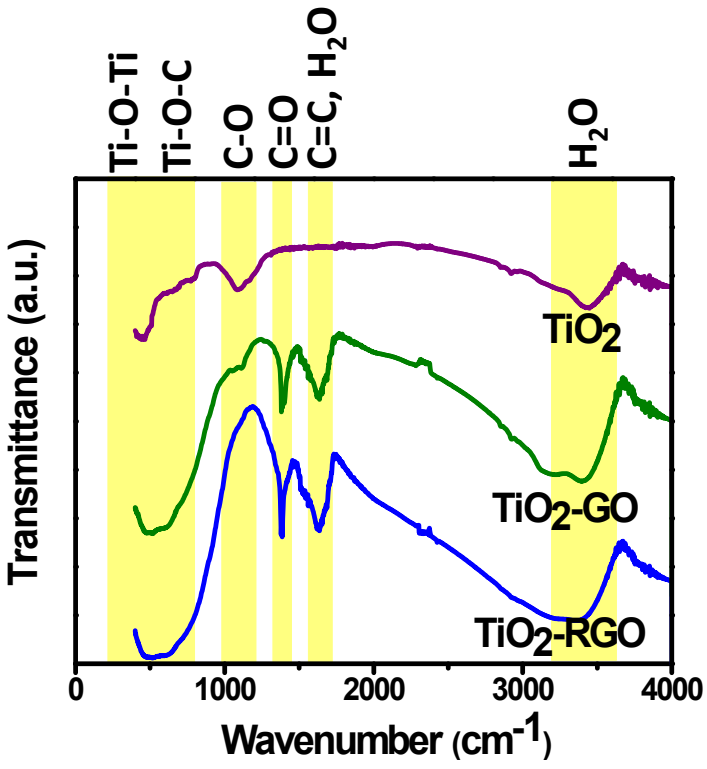

Figure S3. FTIR spectra of pure TiO_2, TG and TR.

Photoluinescence Spectra and Interpretation.

Further, the photoluminescence is frequently employed to study the surface structure and excited state of a semiconductor [9]. After irradiation of the semiconductor, electron–hole pairs are generated and subsequently-radiative recombination takes place, resulting in photoluminescence. Figure S3 shows the photoluminescence spectra of pure TiO_2 nanopowder, TG and TR composites. The emission peak of TiO_2 in TG and TR was slightly broadened and quenched in the range from 350 nm to 500 nm. The reduced emission intensity indicates that the electron transfer from the conduction band of TiO_2 to the GO or RGO sheets, resulting in enhanced photocatalytic activity [10]. This corresponds to an efficient charge separation within TG and TR, which is a needed requirement for a photocatalyst. Due to the retardation of electron–hole recombination, the number of holes participating in the catalytic reaction resulting in more free radicals which decompose MB dye more efficiently.

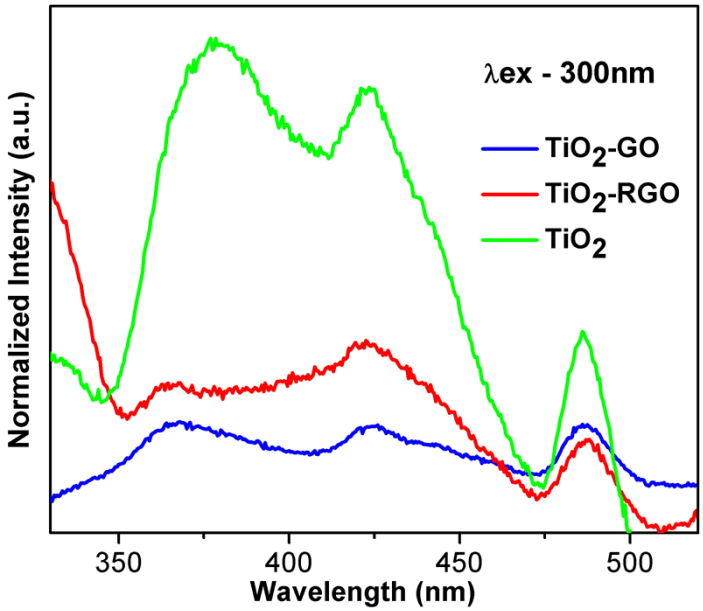

Figure S4. The photoluminescence spectra (PL) of as synthesized TiO_2 nanopowder, TG and TR composites.

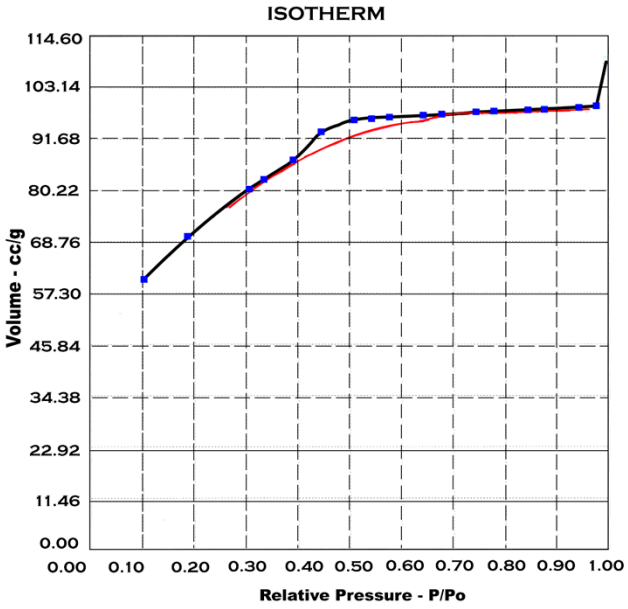

Figure S5. Nitrogen adsorption–desorption isotherm of as synthesized TiO2 nanopowder.

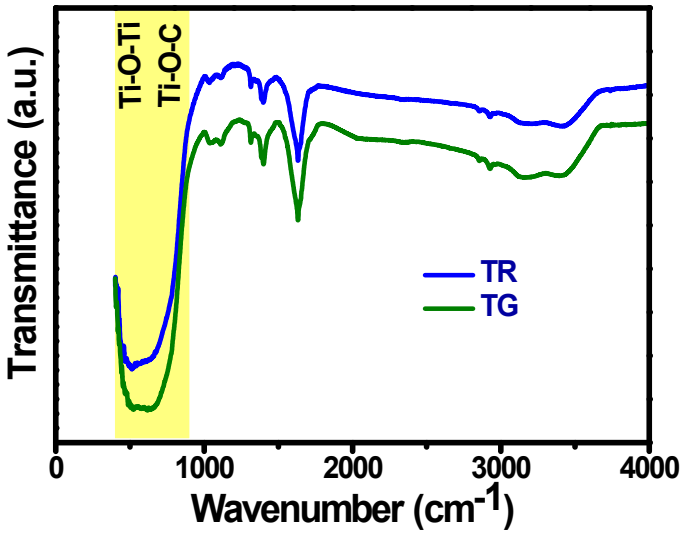

Figure S6. FTIR spectrum of TG and TR after photocatalytic test.

Explanation of the Dependence of Photodegradation Efficiency and Rate Constant on varying Weight % of TiO_2 in Composites:

The effect of decreased ratio of TiO_2: GO/RGO on rate constant of photo degradation of MB (k), of both TG and TR is similar, resulting in increased k value for both. The k value in our TiO_2 nanopowder

over GO/RGO matrix system with MB as degrading specie can be analytically expressed as,

$k = f \times g \times h(\propto_1, \propto_2)$ (1) where f = No. of electrons available for the degrading species at the surface of matrix were the redox reaction takes place,

g = The ability of the matrix to adsorb the degrading species on its surface, and

h = Electron transfer coefficient from TiO_2 to degrading specie; itself a function of $\propto_1$= electron mobility coefficient from TiO_2 to matrix, and $\propto_2$= electron mobility coefficient from matrix to degrading species.

f will depend on number of effective charge carriers (evading recombination) generated by TiO_2 on irradiation which will depend on TiO_2 amount.

$\therefore f(TG1) \approx f(TR1) > f(TG2) \approx f(TR2)$ (2) Similarly with greater functional groups in GO compared to RGO for same area, hence more adsorbtion or locking up of MB on GO would occur compared to RGO,

$\therefore g(TG) > g(TR)$ (3)

$g(TG2) > g(TG1), g(TR2) > g(TR1)$ (4) The synergistical interactions between TiO_2 and matrix would influence $\propto_1$ of the composites, while the conductivity of the matrix would affect the $\propto_2$. Since stronger interaction of TiO_2 with RGO is reported,[11] which also has greater conductivity than GO hence,

$\propto_1(TR) > \propto_1(TG)$ (5)

$\propto_2(TR) > \propto_2(TG)$ (6)

$and \propto_2(TR2) > \propto_2(TR1), \propto_2(TG2) > \propto_2(TG1)$ (7)

$\propto_1(TR2) > \propto_1(TR1), \propto_1(TG2) > \propto_1(TG1)$ (8) The equation 7 and 8 depends on the no. of stacks of GO/RGO present, as beyond a point the matrix would show saturation. GO with low conductivity would be most affected by this and show early saturation for both $\propto_1 and \propto_2$ beyond certain number of stackings ie amount of GO.

With above theoretical analysis, the results in **fig. 6** showing variation in rate constant become clear. The increase in g and h contribution in rate constant in case of both TG and TR explains the dominance in k value of all our as synthesized composites over bare TiO_2 nanopowder. Further with decreasing TiO_2:GO/RGO ratio, the increase in g and h factor (equation 4 & 7) in both TG and TR, more than compensates for the decrease in f for both (equation 2). Even if saturation of $\propto_1 and \propto_2$ might have occurred for TG, increase in g (from equation 4) compensates it. Hence k value increases with drop in TiO_2:GO/RGO ratio for both TG and TR. The greater increasing slope in case of TR (from TR1 to TR2) than TG (from TG1 to TG2) might have the reasoning based on the more dominated increase of $\propto_1 and \propto_2$ of TR over TG (equation 5 & 6, not ignoring the possibility of saturation in $\propto_1 and \propto_2$ in case of TG2), compared to the decrease in g factor of TR over TG (equation 3).

F**igure 6** also showcases the comparison in photodegradation efficiency of the composites and bare TiO_2 nanopowder. Two factors affecting the efficiency would be:

1) no of charge carriers generated by TiO_2 powder on top of matrix of GO/RGO on irradiation and

2) the interactions between TiO_2 and the matrix beneath (confirmed by DFT calculation, FT-IR and PL spectra) which increases the photodegradation efficiency by controlling the recombination of charge carriers in TiO_2, aided by good conductivity through matrix of GO/RGO.

Astonishingly the graph (**fig. 6**) makes it evident that opposite behavior of photodegradation efficiency in response to decreased TiO_2:GO/RGO ratio is observed in TG (TG1 > TG2) and TR (TR2 > TR1). This can be explained as follows: with decreasing amount of TiO_2, less charge carriers are generated in both TG2/TR2 compared to TG1/TR1. The increase or decrease in overall efficiency hence depends on how well the increased interaction (hindering recombination of charges) and conductivity due to matrix in case of TG2/TR2 over TG1/TR1, can compensate the loss in no of net charge carriers, without attaining the saturation limit. Clearly from the graph, efficiency of TR2 is greater than TR1. This might be explained by the much increased conductivity and synergistically interactions offered by

RGO without saturation, more than compensating the loss in net amount of generated charge carriers, due to lower TiO_2 amount in TR2 than TR1. In contrast to TR behavior, efficiency of TG1 is greater than TG2. The possible explanation, can be the less conductivity of GO (compared to RGO) and saturation in the interactions of TiO_2 with matrix attained around this amount of GO, together failing to overcome the loss in net amount of charge carriers, thereby resulting in loss of efficiency. Apart from the above comparative analysis, the results compel us to cognizant the outstanding optimized response achieved in case of TR2 composite. The photocatalytic efficiency is found to be optimum for TR2-P3 with startling results. Commendable 97.59% MB degradation is recorded within 60 min, while it only 75.7% degradation occurred for TG2-P1 catalyst over the same period of time (**Fig. 5c**).

Reference

[S1] A.C. Ferrari, *Solid State Comm*., 2007,**143**, 47-57.

[S2] A. Ferrari, J. Meyer, V. Scardaci, C. Casiraghi, M. Lazzeri, F. Mauri, S. Piscanec, D. Jiang, K. Novoselov and S. Roth, *Phys. Rev. Lett*., 2006, **97**, 187401-187404.

[S3] V. Lee, L. Whittaker, C. Jaye, K.M. Baroudi, D.A. Fischer and S. Banerjee, *Chem. Mater.*, 2009, **21**, 3905-3916.

[S4] W. Zhang, Y. He, M. Zhang, Z. Yin and Q. Chen, J. Phys. D: *Appl. Phys*., 2000, **33**, 912-916.

[S5] A. Maira, J. Coronado, V. Augugliaro, K. Yeung, J. Conesa and J. Soria, *J. Catal*., 2001, **202**, 413-420.

[S6] V. Kumar, S. Srivastava, S. Umrao, R. Kumar, G. Nath, G. Sumana, P. S. Saxena and A. Srivastava, *RSC Advances,* 2014, **4,** 2267-2273.

[S7] S. Sakthivel, and H. Kisch, *Angew. Chem. Int. Ed.*, 2003, **42**, 4908.

[S8] G. Williams, B. Seger and P.V. Kamat, ACS Nano, 2008, 2, 1487-1491.

[S9] Y. Yao, G. Li, S. Ciston, R.M. Lueptow and K.A. Gray, *Environ. scie. & tech.*, 2008, **42**, 4952-4957.

[S10] J. Liu, H. Bai, Y. Wang, Z. Liu, X. Zhang and D.D. Sun, *Adv. Func. Mater.*, 2010, **20,** 4175-4181.

[S11] J. P. Perdew, J. A. Chevary, S. H. Vosko, K. A. Jackson, M. R. Pederson, D. J. Singh and C. Fiolhais, *Phys. Rev. B*, 1992, **46**, 6671-6687.